

Preparation and luminescence of bulk oxyfluoride glasses doped with Ag nanoclusters

V. K. Tikhomirov^{1,*}, V. D. Rodríguez², A. Kuznetsov¹, D. Kirilenko³, G. Van Tendeloo³,
and V. V. Moshchalkov¹

¹ INPAC-Institute for Nanoscale Physics and Chemistry, Katholieke Universiteit Leuven, Belgium

² Departamento de Física Fundamental y Experimental, Electrónica y Sistemas, Universidad de La Laguna, Tenerife, Spain

³ EMAT, Electron Microscopy for Materials Science, University of Antwerpen, Belgium

*Victor.Tikhomirov@fys.kuleuven.be

Abstract: Bulk oxyfluoride glasses doped with Ag nanoclusters have been prepared using the melt quenching technique. When pumped in the absorption band of Ag nanoclusters between 300 to 500 nm, these glasses emit a very broad luminescence band covering all the visible range with a weak tail extending into the near infrared. The maximum of the luminescence band and its color shifts to the blue with a shortening of the excitation wavelength and an increasing ratio of oxide to fluoride components, resulting in white color luminescence at a particular ratio of oxide to fluoride; with a quantum yield above 20%.

©2010 Optical Society of America

OCIS codes: (160.4236) Nanomaterials; (250.5230) Photoluminescence; (160.2750) Glass and other amorphous materials.

References and links

1. Z. Shen, H. Duan, and H. Frey, "Water-soluble fluorescent Ag nanoclusters obtained from multiarm star poly(acrylic acid) as molecular hydrogel templates," *Adv. Mater.* **19**(3), 349–352 (2007).
2. I. Díez, M. Pusa, S. Kulmala, H. Jiang, A. Walther, A. S. Goldman, A. Müller, O. Ikkala, and R. Ras, "Color tuneability and electrochemiluminescence of silver nanoclusters," *Angew. Chem. Int. Ed.* **48**(12), 2122–2125 (2009).
3. R. J. T. Houk, B. W. Jacobs, F. El Gabaly, N. N. Chang, A. A. Talin, D. D. Graham, S. D. House, I. M. Robertson, and M. D. Allendorf, "Silver cluster formation, dynamics, and chemistry in metal-organic frameworks," *Nano Lett.* **9**(10), 3413–3418 (2009).
4. W. W. Guo, J. P. Yuan, Q. Z. Dong, and E. K. Wang, "Highly sequence-dependent formation of fluorescent silver nanoclusters in hybridized DNA duplexes for single nucleotide mutation identification," *J. Am. Chem. Soc.* **132**(3), 932–934 (2010).
5. H. X. Xu, and K. S. Suslick, "Sonochemical synthesis of highly fluorescent ag nanoclusters," *ACS Nano* **4**(6), 3209–3214 (2010).
6. L. Maretti, P. S. Billone, Y. Liu, and J. C. Scaiano, "Facile photochemical synthesis and characterization of highly fluorescent silver nanoparticles," *J. Am. Chem. Soc.* **131**(39), 13972–13980 (2009).
7. M. Ferrari, F. Gonella, M. Montagna, and C. Tosello, "Detection and size determination of Ag nanoclusters in ion exchanged soda-lime glasses by waveguide Raman spectroscopy," *J. Appl. Phys.* **79**(4), 2055–2059 (1996).
8. M. Eichelbaum, K. Rademann, A. Hoell, D. M. Tatchev, W. Weigel, R. Stöber, and G. Pacchioni, "Photoluminescence of atomic gold and silver particles in soda-lime silicate glasses," *Nanotechnology* **19**(13), 135701 (2008).
9. J. Shen, J. Zheng, J. Zhang, C. Zhou, and L. Jiang, "UV-laser-induced nanoclusters in silver ion-exchanged soda-lime silicate glass," *Physica B* **387**(1-2), 32–35 (2007).
10. G. Nunzi Conti, V. K. Tikhomirov, M. Bettinelli, S. Berneschi, M. Brenchi, B. Chen, S. Pelli, A. Speghini, and G. C. Righini, "Characterization of ion-exchanged waveguides in tungsten tellurite and zinc tellurite Er³⁺-doped glasses," *Opt. Eng.* **42**(10), 2805–2811 (2003).
11. V. D. Rodríguez, V. K. Tikhomirov, J. Méndez-Ramos, A. Yanes, and V. V. Moshchalkov, "Towards broad range and highly efficient down-conversion of solar spectrum by Er³⁺-Yb³⁺ co-doped nano-structured glass-ceramics," *Sol. Energy Mater. Sol. Cells* **94**(10), 1612–1617 (2010).
12. V. K. Tikhomirov, D. Furniss, I. M. Reaney, M. Beggiora, M. Ferrari, M. Montagna, and R. Rolli, "Fabrication and characterization of nanoscale, Er³⁺-doped, ultratransparent oxyfluoride glass-ceramics," *Appl. Phys. Lett.* **81**(11), 1937–1939 (2002).
13. V. K. Tikhomirov, T. Vosch, E. Fron, J. Hofkens, M. Van der Auweraer, V. V. Moshchalkov, Catholic University Leuven, are preparing a manuscript to be called "Luminescence lifetimes in glass doped with Ag nanoclusters."

14. Z. Wu, and R. Jin, "On the ligand's role in the fluorescence of gold nanoclusters," *Nano Lett.* **10**(7), 2568–2573 (2010).
15. P. Boutinnand, A. Monnier, and H. Bill, "Luminescence mechanisms of Ag⁺ cubic centers in strontium fluoride crystals," *J. Phys. Condens. Matter* **6**(42), 8931–8947 (1994).
16. J. C. Pickering, and V. Zilio, "New accurate data for the spectrum of neutral silver," *Eur. Phys. J. D* **13**(2), 181–185 (2001).
17. S. Hull, "Superionic crystal structures and conduction processes," *Rep. Prog. Phys.* **67**(7), 1233–1314 (2004).
18. Y. Dai, X. Hu, C. Wang, D. Chen, X. Jiang, C. Zhu, B. Yu, and J. Qiu, "Fluorescent nanoclusters in glass induced by an infrared femtosecond laser," *Chem. Phys. Lett.* **439**(1-3), 81–84 (2007).
19. E. Borsella, F. Gonella, P. Mazzoldi, A. Quaranta, G. Bataglin, and R. Polloni, "Spectroscopic investigation of silver in soda-lime glass," *Chem. Phys. Lett.* **284**(5-6), 429–434 (1998).
20. C. Strohhofner, and A. Polman, "Silver as a sensitizer for erbium," *Appl. Phys. Lett.* **81**(8), 1414–1416 (2002).
21. M. Mattarelli, M. Montagna, K. Vishnubathla, A. Chiasera, M. Ferrari, and G. C. Righini, "Mechanisms of silver to erbium energy transfer in silicate glasses," *Phys. Rev. B* **75**, 125102 (2007).

1. Introduction

Photoluminescence of silver (Ag) *nanoclusters* embedded in different hosts has recently been attracted substantial interest because of the promising applications in optical nanolabels, visible light sources, optical recording, and other, e.g. [1–6 and refs therein]. In particular, the Ag nanoclusters have been embedded at the surface of some sodium (Na) containing *oxide* glasses, such as silicate [7–9] and tellurite (TeO₂) [10] glasses, by means of ion exchange Ag→Na techniques at elevated temperatures, and their optical properties have been studied [7–10 and refs therein].

Here, we report on the preparation of *oxyfluoride glass* doped with Ag nanoclusters, which have been spontaneously created within this glass on its casting without any further heat treatment steps. The glassy state of this material provides the options of its preparation in film and fiber forms; and indeed we have pulled an unstructured fiber in air atmosphere with an attenuation loss of several dB/cm. The structure of the glass and Ag nanoclusters has been characterized by means of transmission electron microscopy. The luminescence band of Ag nanoclusters expands from 400 to 1000 nm and it is most efficiently excited with UV-violet light at about 325 to 425 nm. These features point out an option to use this luminescence in screen monitors, where a glow is excited with a UV light source, while the red, green and blue components of the glow may be selected by the color filters. Other applications may be in the white light and visible light generation, CW laser sources tunable across the visible range of the spectrum, and in down-conversion of the solar spectrum for enhancement the efficiency of the Si solar cells; e.g. in [11 and refs therein].

2. Experimental and results

2.1 Preparation of bulk glass doped with Ag nanoclusters

The oxyfluoride glass has been prepared by batching the constituent oxides and fluorides according to the formula 33(SiO₂)9.5(AlO_{1.5})32.5(CdF₂)19.5(PbF₂)5.5(ZnF₂), mol%, somewhat similar to the formula of the oxyfluoride glass developed in [12]. This oxyfluoride glass will be called further in the text the *basic glass*. The proportion of oxide to fluoride has been increased in some samples; this will be noted in the text where appropriate. When preparing the batch, we have also added some wt% of the AgNO₃, and in particular cases 3.5 mol% of YbF₃, substituting for CdF₂. All reagents were of highest purity supplied by Alfa-Aesar. The batch was melted at about 1000 to 1300°C in a Pt crucible; the melting temperature was increased with an increasing proportion of the oxides. The melts were casted into a mold preheated to 350°C. Afterwards, the mould was allowed to cool to room temperature, while placed into another furnace, with a cooling rate about 10°/min. No further intentional heat-treatment steps were undertaken in the preparation of these glasses. The resulting pieces of the glass were normally of 4 × 1 × 0.3 cm³ in size, according to the shape of the mold. Afterwards, these glass pieces were polished and cut in smaller pieces for optical and structural characterization.

2.2 Structure of samples

Figure 1 shows the photos of several glass samples in daylight, Fig. 1(a), and UV, Fig. 1(b), ambient light. The Ag doped glasses, (samples 1, 2, 3), are homogeneously transparent and have a light yellow color, while the undoped glass, (sample 4), is completely transparent in the visible. Under UV illumination, the undoped glass emits a weak blue luminescence, while doping with Ag results in orders of magnitude stronger yellow luminescence, which increases with the Ag doping level (from sample 2 to 1), and becomes white in the glass with an enhanced oxide content (sample 3).

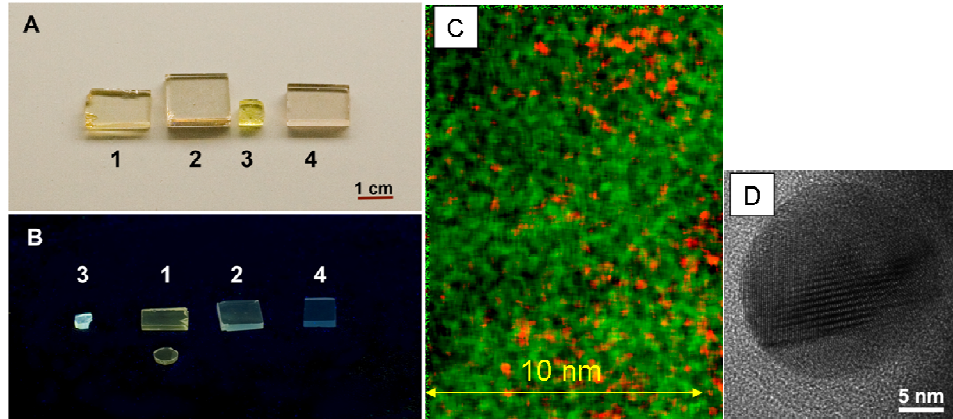


Fig. 1. (a) Daylight picture of as-prepared glass samples: **1** is the basic glass doped with 10 wt% AgNO_3 ; **2** is the basic glass doped with 1 wt% AgNO_3 ; **3** is the oxygen-enriched glass $51(\text{SiO}_2)14(\text{AlO}_{1.5})22.5(\text{CdF}_2)10(\text{PbF}_2)2.5(\text{ZnF}_2)$, mol%, doped with 5 wt% AgNO_3 ; **4** is the undoped basic glass. b) Luminescence image of the same glass samples, marked respectively, excited with a UV lamp CAMAG at 366 nm. c) Energy filtered transmission electron microscope image of a piece of the basic glass doped with 1 wt% AgNO_3 and 3.5 mol% of YbF_3 : the red color represents Ag and the green color represents Yb, respectively. d) TEM image of a single Ag nanoparticle grown by intentional heat-treatment of the basic glass doped with 1 wt% AgNO_3 : the glass was treated at 350°C for 1 hour.

The nano-structure of glasses has been studied by means of X-ray diffraction (XRD) and transmission electron microscopy (TEM). Elemental maps for Ag *aggregates/nanoclusters* have been obtained with an energy filtered TEM (EFTEM) using the $\text{Ag-M}_{4,5}$ inner-shell edge in the electron energy loss spectrum (EELS) of the sample. Elemental maps for Yb were obtained using the $\text{Yb-N}_{4,5}$ inner-shell edge in EELS. The background in the EELS data has been subtracted using the three-window method, by measuring the background at the low energy side of the corresponding inner-shell edge. Figure 1(c) shows an EFTEM image of a fragment of the glass co-doped with Ag and Yb.

We found that co-doping with Yb stabilizes the glass against electron beam damage in the TEM, while the glass doped with only Ag was less stable under the electron beam. This is perhaps due to an extra aggregation of Ag^+ ions into the area of the negative charged electron beam. As it will be seen in Fig. 4, co-doping with Yb does also affect the emission spectrum of Ag nanoclusters. This, together with the stabilization of the glass against the electron beam, is an indication that an introduction of Yb^{3+} in the glass matrix restricts the growth of the Ag nanoclusters and therefore quenches the red tail of the luminescence band of the Ag nanoclusters. This restriction of the growth however is not substantial, as it will be discussed further.

Ag signals from the glass observed in Fig. 1(c) stem from tiny Ag *nanoclusters/aggregates* with an average size below 1 nm. Remarkably, the XRD pattern of this glass showed only broad amorphous halos, similar to the halos shown in Fig. 2 of Ref [12]. for the same oxyfluoride glass, indicating an absence of larger size *crystalline nano-phases or crystalline micro-phases* in this glass. Obviously, the XRD technique is not suitable for the detection of

such tiny Ag nano-aggregates, as shown in Fig. 1(c), because the XRD peaks of such small entities are too broad for the detection in the respective XRD patterns.

Differential thermal analysis (DTA) curves of the basic glasses doped with different amounts of Ag indicated their glass transition temperature T_g at about 370° C, again similar to the one in [12], where the same oxyfluoride glass host has been investigated. Some pieces of the basic glass doped with 1 wt% AgNO₃ have been intentionally *heat treated* at temperature of 300 to 350°C, i.e. below its glass transition temperature, T_g , to avoid softening of the glass on the heat treatment. In the intentionally heat treated at 350°C glass sample, we have detected the dispersed *spherical Ag nanoparticles* with a mean diameter of about 20 nm, one of them is shown in Fig. 1(d), for example. The XRD patterns of this intentionally heat treated glass sample showed crystalline peaks corresponding to the face centered cubic phase of Ag. Having measured the half height width of the silver XRD peak at about $2\theta = 38^\circ$ and using the Scherrer formula, we have calculated the average diameter of Ag nanoparticles to be about 20 nm, in agreement with TEM data.

2.3 Emission and excitation spectra

The spectral response of the set-up has been taken into account in all below shown spectra, while an extended Hamamatsu photomultiplier has been used for detection of the emission. The emission and excitation spectra of the basic glass doped with 5 wt% of AgNO₃ are shown in Fig. 2.

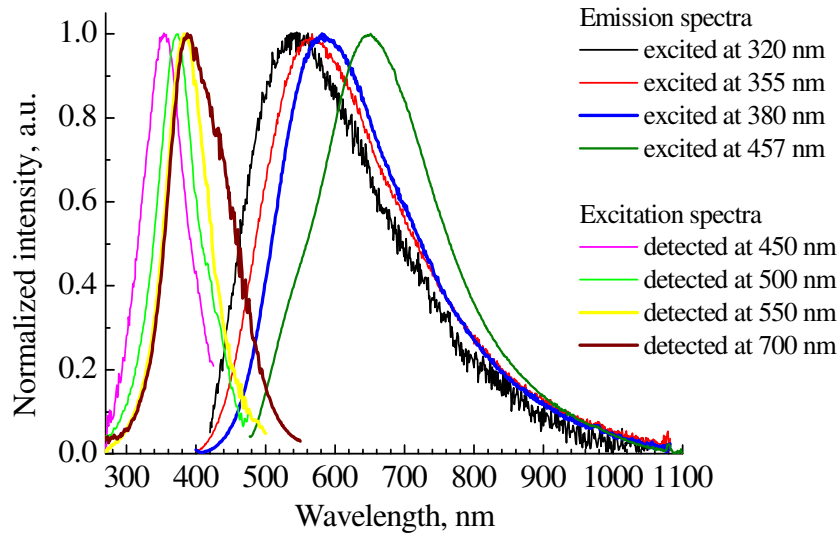


Fig. 2. Normalized emission and excitation spectra of the basic glass doped with 5 wt% AgNO₃. Emission and excitation wavelengths are post-signed, respectively.

The emission in Fig. 2 comes from the Ag dopants, since the same basic undoped glass, containing no Ag, shows a very different luminescence, as depicted in Fig. 1(b) and Fig. 3. In particular, the luminescence of undoped glass cannot be excited at wavelengths longer than 380 nm, and at the wavelengths at which it can be excited, its maximum integrated intensity is orders of magnitude lower than the maximum integrated intensity in the basic glass doped with Ag; this can be seen, e.g. in photos of Fig. 1(b). Moreover, the most intense emission band of the Ag dopants in Fig. 2 is observed at an *optimum* excitation wavelength of 380 nm, while the luminescence of the undoped glass host is not excited at 380 nm, see Fig. 3.

When excited at the optimum wavelength of about 380 nm, the resulting emission spectrum, further called an *optimized emission spectrum* of Ag dopants, peaks at about 580 nm, i.e. in the yellow part of the spectrum. The excitation spectrum, which is obtained by detection at 580 nm emission wavelength, will be further called an *optimized excitation*

spectrum. The position and shape of the emission and excitation spectra in Fig. 2 do match the earlier reported respective spectra of *Ag nanoclusters* [1–6]. Moreover, it was detected in [13] that the lifetime of the Ag emission band, at the maximum of the optimized emission spectrum, equals to 2.6 ns, which agrees with the lifetime of Ag nanoclusters dispersed in other media [1–6].

The shortening of the excitation wavelength in Fig. 2, from 457 to 320 nm, results in a blue shifting of the respective emission spectrum. A similar shifting with excitation wavelength has been detected in semiconductor quantum dots, and it has been related to the size-selective excitation of the quantum dots. Therefore, we conclude that the short wavelength part of the Ag emission spectrum corresponds to the emission by smaller size Ag nanoclusters, while the long wavelength part corresponds to emission by larger size nanoclusters, and the largest light emissive Ag nanoclusters emit in the red-to-infrared tail of the Ag emission band down to 1100 nm (Fig. 2). When the size of Ag nanoclusters reaches a critical value, they apparently cease to emit, perhaps because they are acquiring bulk silver metal properties, in particular an absence of luminescence. With increasing the Ag doping level, the emission spectra are shifted to the red at the same excitation wavelength indicating that the average Ag nanoclusters size does increase with the Ag doping.

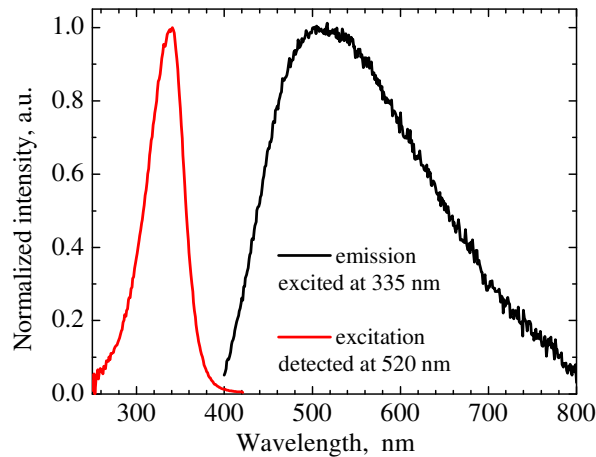


Fig. 3. Normalized emission and excitation spectra of the undoped basic glass, as post-signed. The emission spectrum does not shift appreciable with change of the excitation wavelength.

Figure 4 illustrates an effect of Yb co-dopant on the spectrum of the glass presented in Fig. 2. It was noted above that co-doping with Yb restricts the growth of the Ag nanoclusters, and indeed we see in Fig. 4 that luminescence of larger Ag nanoclusters, emitting in the red and infrared, has been suppressed, and the maximum of Ag emission shifts to the blue from 580 to 550 nm. In addition, an emission band of Yb^{3+} corresponding to the only *f-f* transition $^2F_{5/2} \rightarrow ^2F_{7/2}$ of Yb^{3+} , appears around 980 nm. This may indicate an electron energy transfer from the larger size Ag nanoclusters to the Yb^{3+} co-dopants.

In principle, the Yb^{3+} might be directly excited at 380 nm, either into its charge transfer *d*-state or due to energy transfer from other atoms involved in the chemical formula of this glass. To check this, we have prepared and compared the *single* Yb^{3+} doped glass and the glass co-doped with the same concentration of Yb^{3+} and Ag; their excitation spectra and the difference between them is shown in Fig. 5. It is seen that indeed, the Yb^{3+} is excited directly in a broad band peaked at about 315 nm in single Yb^{3+} -doped glass, but Ag co-dopants broaden the excitation band of Yb^{3+} and shift the excitation maximum to 345 nm.

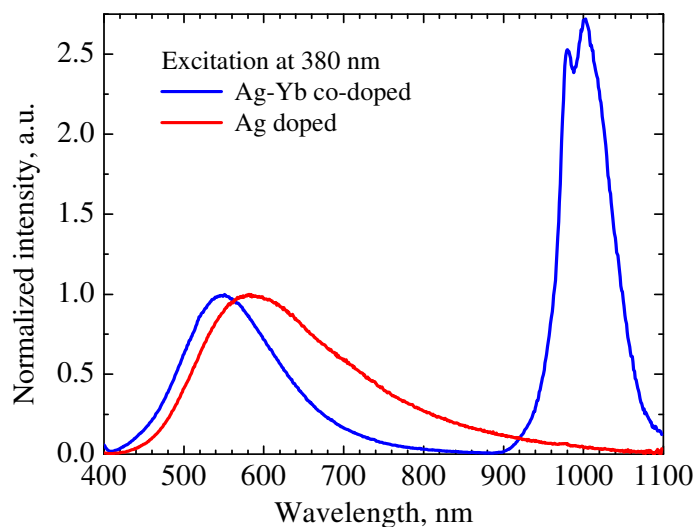


Fig. 4. Normalized emission spectra of the basic glass doped with 5 wt% AgNO_3 (red curve) and the basic glass co-doped with 5 wt% AgNO_3 and 3.5 mol% YbF_3 (blue curve).

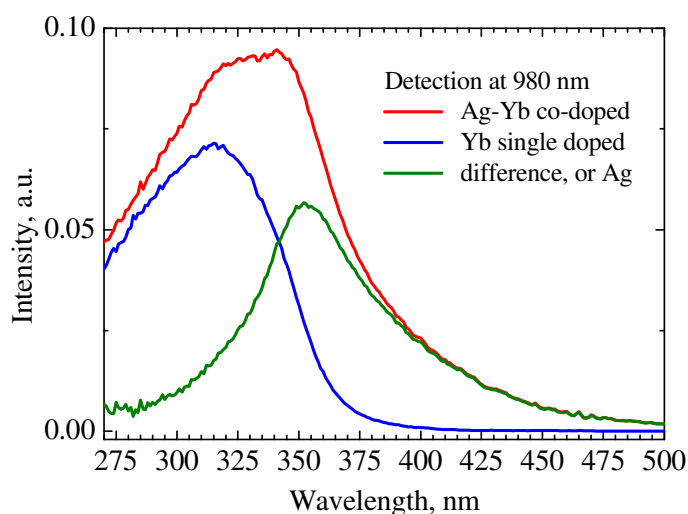


Fig. 5. Excitation spectra of 980 nm emission band of Yb^{3+} in the basic glass single doped with 3.5 mol% YbF_3 (blue curve) and in basic glass co-doped with 3.5 mol% YbF_3 and 1 wt% of AgNO_3 (red curve). The green curve shows their difference.

The difference spectrum in Fig. 5 peaks at 355 nm and it is similar to the excitation spectrum of the Ag nanoclusters in Fig. 2, when detected at 450 nm, i.e. with the excitation spectrum of smaller Ag nanoclusters. This indicates that the excited smaller Ag nanoclusters transfer some part of the electron excitation to Yb^{3+} , perhaps via nanoclusters of a larger size, which emit in the red and near-infrared (Fig. 2 and Fig. 4), overlapping with the emission band of Yb^{3+} .

Figure 6 shows the optimized emission and excitation spectrum of the glass, sample 3 in Fig. 1(b), which is enriched with oxide components. The most intense excitation in this glass

occurs at 335 nm with a resulting emission spectrum peaked at 520 nm. Note that optimized emission and excitation spectra for this oxygen-enriched glass are shifted to the blue compared to the respective spectra in Fig. 2. Such emission spectrum has red, green and blue components; therefore the color of this emission is near to white. We have estimated a quantum yield for emission of this sample at about 20% using the integration sphere detection, when excited at about 360 nm. Since the maximum of excitation of this glass peaks at the shorter wavelength of 335 nm, then the yield could be even higher when excited at the wavelengths closer to 335 nm. A shoulder at 315 nm can be seen in the excitation spectrum in Fig. 6. It may indicate that the emission of Ag nanoclusters can be excited by pumping and energy transfer from the glass host in oxygen-enriched glass hosts.

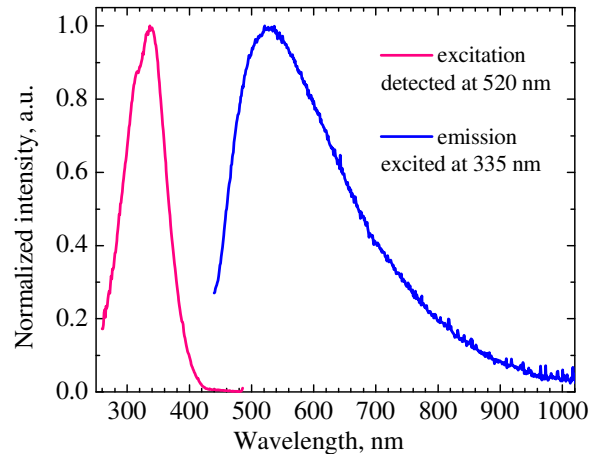


Fig. 6. Optimized emission and excitation spectra of an oxygen-enriched glass $51(\text{SiO}_2)14(\text{AlO}_{1.5})22.5(\text{CdF}_2)10(\text{PbF}_2)2.5(\text{ZnF}_2)$, mol%, doped with 5 wt% AgNO_3 (sample 3 in Fig. 1 (b)).

3. Discussion

Although the luminescence of metal nanoclusters in a variety of hosts has been investigated for a few years, the mechanism for this luminescence has not been completely understood, e.g. [14 and refs therein].

The luminescence spectrum of single Ag^+ ion lies at about 300 nm and its half height width is about 25 nm [15 and refs therein]; this is different principally from the Ag luminescence spectra in our glasses (Figs. 2,4,6), indicating that in these glasses, the Ag luminescence stems from Ag nanoclusters. At the moment, it is difficult to name precisely the number of Ag atoms in these nanoclusters and this will be addressed in the following work dealing with computer simulations of Ag nanoclusters electronic structure. EFTEM and XRD techniques, Fig. 1(c), point out an angstrom scale of the nanoclusters and that some distribution of the cluster sizes takes place, which fortunately results in broadening the luminescence spectra. Comparing the emission spectra, we also can conclude that an average size of Ag nanoclusters decreases with co-doping of these glasses by Yb^{3+} , Fig. 4, in agreement with EFTEM data Fig. 1(c); and also with increasing oxides content in the glass composition, Fig. 1(b) and Fig. 6. The red-infrared vanishing tail of the luminescence band in the single Ag-doped glasses, Fig. 2 and Fig. 4, indicates that the largest Ag nanoclusters cease to emit, perhaps because of acquiring the properties of metallic silver.

The simplified energy level diagram suggested in Fig. 7 illustrates the excitation and emission transitions in Ag nanoclusters and accounts for the observed large Stokes shift of the luminescence (Figs. 2,4,6). While the ground state of the silver atom is fixed, the excited state

may be a matter of controversy, because the Ag atom has a rich number of excited states, e.g. in [16 and refs therein]. We follow here the notations of the work [15], where luminescence of the prototype single Ag^+ ions in a cubic site of a fluoride crystal has been studied and modeled. The detailed diagram for Ag nanoclusters will be addressed in the following work.

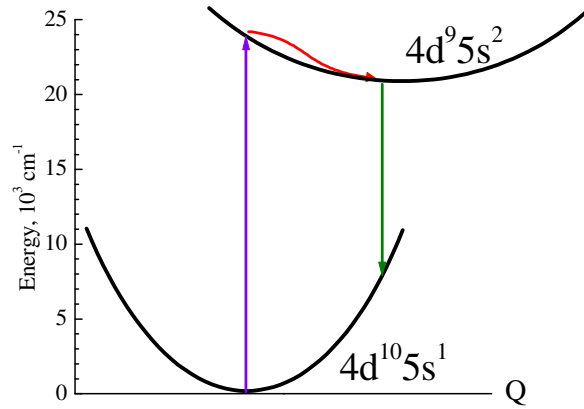
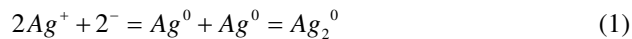


Fig. 7. The simplified energy configuration diagram illustrates the excitation and emission transitions in Ag nanoclusters by straight lines. The wavy red curve corresponds to relaxation in the excited state between the sub-levels of a single nanocluster, and energy transfer between separated nanoclusters, whose energy splitting depends on the parameters of the crystalline field around Ag nanoclusters sites, as e.g. in [15].

It was mentioned in the introduction that up to now the Ag nanoclusters were embedded only in oxide glasses and only at their surface by means of ion exchange $\text{Ag} \rightarrow \text{Na}$ techniques at elevated temperature. A homogeneous doping of the *bulk oxide glass* with Ag nanoclusters seemed to be impossible [7-10 and refs therein]. The oxyfluoride glass presented in this work has a substantial *fluoride* component, which apparently makes it possible to dope the glass homogeneously with Ag nanoclusters. Indeed, the Ag atoms in these oxyfluoride glass network become mobile already at 300 to 350°C, as proven by the heat treatment induced condensation of Ag atoms in 20 nm diameter silver nanoparticles depicted in Fig. 1(d), while in oxide glasses the Ag atoms become mobile at substantially higher temperatures above 500°C [7–10]. The high mobility of the Ag atoms in the fluoride network component perhaps assures a static homogeneous dispersion of Ag nanoclusters in this oxyfluoride glass network.

The intrinsic property of alkali halides, including PbF_2 and CdF_2 fluorides (which are the substantial components of the oxyfluoride glasses studied here), are the F^- vacancies, otherwise called color centers, or F-centers, e.g. in review [17 and refs therein], where an electron substitutes onto the place of an F^- . These vacancies/centers are statistic homogeneously dispersed across the host and they are obvious attractors for Ag^+ ions. Moreover, at elevated temperatures, the F-centers *intrinsically* condense in nanoclusters consisting of two and more F-centers [17], which then will be an obvious nucleation center for the Ag-nanoclusters consisting of the respective amounts of the Ag^+ ions, which then will also be statistic homogeneously dispersed in the host as the F-centers are. The high ionic conductivity of fluorides, especially of PbF_2 [17], helps to create nanoclusters of F-centers, and the known high ionic conductivity of Ag^+ in silver halides helps to trap the Ag nanoclusters on nanoclusters of F-centers. The charge compensation mechanism in case of trapping two Ag^+ ions near a nanocluster of two F-centers (or two electrons $^-$ on place of two F^- ions) can be described by Eq. (1) resulting in the formation of a neutral Ag_2^0 nanocluster:



The two Ag^+ ions may substitute either of Cd^{2+} or Pb^{2+} cations, as in [15], and nearby cation vacancies that are typical in PbF_2 and CdF_2 hosts, page 1242 in [17]. Note that Ag is next to

Cd atom in the periodic table, making a substitution especially easy, and the concentration of the F⁻ nanoclusters above 1% in PbF₂ and CdF₂ (page 1241 in [17]), matches the concentration of Ag dopants in these glasses allowing an accommodation of all the Ag⁺ dopant ions.

The nanoclusters of F-centers and the resulting Ag nanoclusters might already be created in the melt of the glasses because we noted that the silver has not been dispersed in the glass melt, and even did precipitate on the bottom of the crucible, when melted in particular crucibles, e.g. in a silica crucible.

Finally, the emission spectra of Ag⁺ monomers and nanoclusters have been investigated in soda-lime based oxide glass hosts [18,19] and the spectral positions of the respective identified emission bands differ substantially from the Ag emission band in this work, indicating that the surrounding of Ag nanoclusters in our oxyfluoride glass is not of oxide origin.

The energy transfer mechanism where silver clusters play the role of sensitizer for the luminescence of rare earth ions, as of Yb³⁺ in our case, without plasmonic contribution, has been considered earlier in Refs [20,21]. and will be refined in the following work.

4. Conclusion

Bulk oxyfluoride glass doped with Ag nanoclusters has been prepared. The glassy state of this material suggests a possibility to prepare it in film or fiber form. When optically pumped in the UV-blue absorption band of the Ag nanoclusters, this glass emits a broad luminescence band of Ag nanoclusters covering the whole visible range; its quantum efficiency can be above 20%. This emission band has a potential for application in broad band visible light sources, CW lasers tunable across the whole visible range, and panel displays based on selective filtering of red, green and blue parts from the emission band of Ag nanoclusters.

Acknowledgement

We are grateful to the Methusalem Funding of Flemish Government for the support of this work. We are grateful to E. Fron, Chemistry Department, KU Leuven, for the photographs of samples in Figs. 1(a),(1b). We are grateful to Dr. J. Méndez-Ramos (Universidad de La Laguna, Spain) for help in luminescence measurements. We also thank Ministerio de Ciencia e Innovacion for financial support (MAT2009-12079).